

## Preparation of CdO-TiO<sub>2</sub> Nanocomposite Thin Films and Study Their Structural and Optical Properties

Ahmed K. Abass

Department of Chemistry, College of Science, University of AL-Qadisiyah, 1753 Dewanyia, Iraq

**Abstract:** Nanocomposite CdO-TiO<sub>2</sub> thin films had been deposited on conductive glass (ITO) at calcination temperatures in the range 350-650°C via. doctor blading method. The structural, morphological, compositional and optical properties have been characterized via XRD, SEM, AFM, EDS and UV-Vis spectroscopy. XRD patterns display the rhombohedral structure and crystalline nature of the films. All films were nanomaterials according to Scherrer equation in XRD analysis. SEM images disclose the homogenous films in the form of densely packed nanoparticles. AFM analysis illustrated that both the surface roughness and grain size increase barely with growing temperature. EDS analysis confirms the presence of oxygen, cadmium and titanium elements with the function of cadmium-rich and titanium-poor. Agreeing with Tauc plots, optical band gaps of CdO-TiO<sub>2</sub> films are envisioned to be 1.25-0.9 eV.

**Key words:** Metal oxide seiconductors, thin films, nanocomposites, nanomaterials, homogenous, cadmium

### INTRODUCTION

Recently, nanostructure semiconductor materials have been the major focus of scientific research due to their uncommon optical, chemical (Kumar *et al.*, 2003), electronic properties and photo electrochemical properties (Chandrasekharan and Kamat, 2000; Peto *et al.*, 2002). Titanium dioxide is one of the extensively used transition-metal oxide materials owing to its various important applications in self-cleaning (Zhang *et al.*, 2004), photocatalysis (Matsumoto *et al.*, 2000), environmental cleanup (Andersson *et al.*, 2002), dyesensitized solar cells (Benko *et al.*, 2003; Karuppuchamy *et al.*, 2002), gas sensors (Rothschild *et al.*, 2003), optical coatings (Watanabe *et al.*, 1999) and purification of air and toxic gases because of its excellent chemical stability, photocatalytic decomposition of organics and contaminants, mechanical hardness, optical transmittance with high refractive index and strong redox ability (Takeda *et al.*, 2001).

Furthermore, the hydrophilic coating (0 water contact angle) has emerged as a new and very attractive application of TiO<sub>2</sub> (Wang *et al.*, 1997; Sakai *et al.*, 2001). Since, the TiO<sub>2</sub> films exhibit heavy amphiphilic properties under Ultraviolet (UV) light irradiation and are transparent in nature, it can be used in various kinds of applications such as self-cleaning and as anti-fogging materials in motor cars, buildings and household glazing (Sakai *et al.*, 2001). Cadmium oxide have been usually used as a transparent conducting oxide thin films due to its distinctive properties such as high transmission

coefficient in the visible range of the electromagnetic spectrum, high electrical conductivity. It has n-type semiconductor and an optical band gap lie between 2.2-2.7 eV depending on the type of technique used and the condition of preparation of technique used (Rusu and Rusu, 2005; Dakhel, 2011; Dakhel and Ali-Mohamed, 2007). These properties make condition thin films very suitable for applications, such as heat mirror, solar cells, antireflection coatings, nonlinear optics and gas sensors (Maity and Chattopadhyay, 2006; Lokhande *et al.*, 2009; Matsubara *et al.*, 2003; Henari and Dakhel, 2008; Srinivasaraghavan *et al.*, 2013).

Perovskite titanates structure ATiO<sub>3</sub> (A = Pb, Eu, Ba, Cd, Ca or Sr) are of immense importance from both a scientific and a practical point of view (Burns and Scott, 1973; Burns, 1974; Burns and Dacol, 1978; Soon *et al.*, 2008; Takesada *et al.*, 2006; Shigenari *et al.*, 2006; Taniguchi *et al.*, 2005; 2007; Uplane *et al.*, 2004). They typically undergo a series of phase transitions as a function of temperature and pressure transitions involving impulsive polarization to form a ferroelectric phase are utilized in a diversity of fields such as transducers, capacitors, waveguides, heat sensors and ferroelectric random access memory (Rabe *et al.*, 2007).

Cadmium titanate, CdTiO<sub>3</sub> is unusual in that both its para-electric and ferroelectric phases have orthorhombic structures whereas for other perovskites exhibiting a ferroelectric phase transition, the paraelectric phase is typically cubic and the ferroelectric phase tetragonal. Under standard conditions, the crystal structure of CdTiO<sub>3</sub> belongs to space group Pnma and can be thought

of as being formed by repeated tilting of the  $\text{TiO}_6$  octahedral units of the ideal cubic perovskite structure (Sasaki *et al.*, 1987). This tilting results (space group  $Pm\bar{3}m$ ) in a zigzag fashion in a decrease in symmetry and increase in size of the unit cell from one formula unit (5 atoms) for the cubic cell to four formula units (20 atoms) for the orthorhombic cell, as illustrated in Figs. At about 85.5 K,  $\text{CdTiO}_3$  suffers a phase transition from the centrosymmetric orthorhombic structure to a non-centrosymmetric structure (Smolenski, 1950; El-Mallah *et al.*, 1987; Sun *et al.*, 1998).

The break in symmetry of the positions of Ti and O ions along the long axis (b axis) and their shift relative to the A cations introduces a dipole moment, so that, the low-temperature phase is ferroelectric while still retaining overall orthorhombic symmetry. Shan *et al.* (2001) performed rietveld analyses of powder X-ray diffraction data at 15 K and concluded that the ferroelectric structure has either  $Pn21a$  or  $P21ma$  symmetry. The two space groups are noncentrosymmetric subgroups of space group  $Pnma$ . The former relates to a softening of the vibrational mode with  $B2u$  symmetry in the parent  $Pnma$  structure while the latter results from a softening of the  $B3u$  mode (Gorshunov *et al.*, 2005). The purpose of this research is synthesis nanocomposites of cadmium oxide with titanium oxide and study the effect of substrate temperature on some structural and optical constants using doctor blading method.

## MATERIALS AND METHODS

**Synthesis of CdO-TiO<sub>2</sub> powder:** Titanium dioxide (anatase, TRONOX) was from Croma-Gesellschaft mbH and Co and cadmium iodide was from Sigma-Aldrich. CdO-TiO<sub>2</sub> nanocomposite was prepared by impregnation method as follows: 2.8519 g of  $\text{CdI}_2$  was dissolved in 100 mL deionized water with vigorous stirring until complete solubility and a homogenous solution reached. Then 1 g of  $\text{TiO}_2$  was put in the above solution with vigorous stirring at 60°C for 6 h. The above precipitant dried in oven at 120°C over night. The dried solid precipitant was grinded in a ceramic mortar and calcined at 450°C for 3 h.

**Synthesis of CdO-TiO<sub>2</sub> nanocomposite thin film:** ITO glass used as the substrates during the deposition process. The substrates were first cleaned in ethanol solution and subsequently ultrasonically washed with distilled water. Substrates were then dried in an oven at 120°C. The CdO-TiO<sub>2</sub> nanocomposite thin film was prepared by the doctor blading method as follows: CdO-TiO<sub>2</sub> paste prepared by blending 1 g of CdO-TiO<sub>2</sub>

with a mixture of 0.5 g Polyethylene Glycol (PEG) and 1.5 mL deionized water in a ceramic mortar with vigorous stirring for 10 min. Then drops of this paste were put on the conducting face surface of ITO glass substrate. The paste was spread by means of glass rod according to the doctor blading method. After that the glass was calcined at different temperatures 350, 450, 550, 650°C in the furnace.

## RESULTS AND DISCUSSION

**XRD analysis:** The XRD diffractograms of CdO-TiO<sub>2</sub> at different calcination temperatures 350-650°C were scanned in the range of  $2\theta$  (10-80) at wavelength 1.54Å. The diffractograms and associated data depict  $2\theta$  for each peak, relative intensity and inter planar spacing (d) and all diffractograms had maxima at position (1 0 4).

The XRD spectra of nanocomposite CdO-TiO<sub>2</sub> films are shown in Fig. 1. All films were polycrystalline had rhombohedral structure with space group  $R\bar{3}$  (148). Three strongest peaks in each temperature at  $2\theta$  positions of 31.03, 34.12 and 46.83°C can be assigned to the planes (1 0 4), (1 1 0) and (0 2 4) planes of the rhombohedral structure (JCPDS Card No. 00-029-0277). In addition to these peaks, another peaks corresponding to (0 0 3), (1 0 1), (0 1 2), (1 0 4), (0 1 5), (1 1 3), (0 2 1), (0 2 4), (1 1 6), (0 1 8), (2 1 1), (1 2 2), (2 1 4), (3 0 0), (1 2 5), (1 0 10), (2 1 7), (0 1 11), (2 2 3) and (1 2 8) planes were observed in all the samples.

XRD peaks were indexed as hexagonal structures, then converted to rhombohedral structure. The lattice and microstructural parameters are shown in Table 1 and 2, respectively

The lattice parameters 'a' and 'c' of the unit cell were evaluated according to the relation where d is the inter planar spacing. All lattice parameter values at different calcination temperatures were calculated according to, (0 0 3) and (1 0 1) planes. The lattice parameter values of all the films showed a very little deviation from the standard values which might be due to small strain introduced in the samples which means that the sample was contain only on Cd, Ti and O atoms as expressed by EDS technique.

The calculated values of microstructural parameters such as strain and dislocation density were presented in table. The crystallite size 'D' of the film increases slightly with increasing calcination temperature. With increased calcination temperature, the density of the nucleation centers decreases and under these circumstances, a small number of centers start to grow, resulting in larger grains.

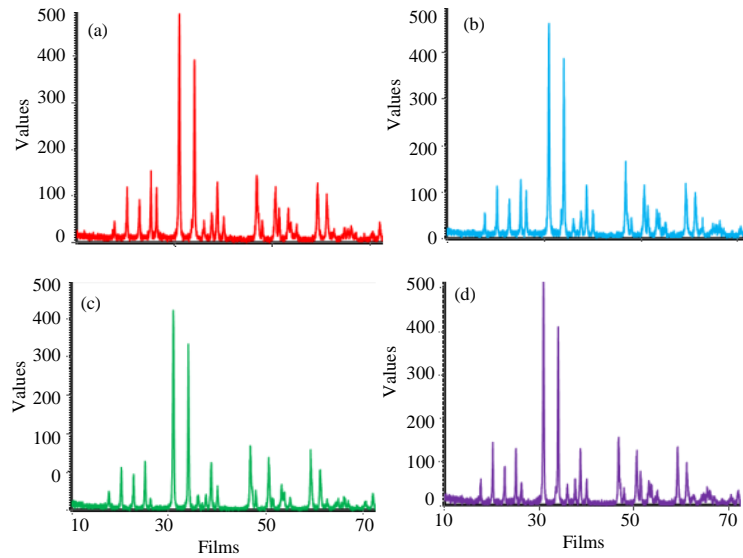


Fig. 1: XRD diffractograms of CdO-TiO<sub>2</sub> nanocomposite thin films at different temperatures (a = 350°C, b = 450°C, c = 550°C, d = 650°C)

Table 1: Lattice parameters of CdO-TiO<sub>2</sub> thin films

Calcination temperature	(°C) a		c		c/a		No. unit cell	Rhombohedral		
	Obs.	Calc.	Obs.	Cal.	Obs.	Calc.		a = b = c	α = β = γ	R. Volume
350	5.2400	5.2568	14.8380	14.9133	2.8320	2.8370	86212	5.8244	53.6512	118.9664
450	5.2400	5.2428	14.8380	14.8441	2.8320	3.5943	88834	5.8004	53.7352	117.7846
550	5.2400	5.2774	14.8380	14.9534	2.8320	2.8335	100420	5.8420	53.7030	120.2238
650	5.2400	6.1317	14.8380	15.0121	2.8320	2.4483	91146	6.1297	60.0218	162.9343

Table 2: Microstructural parameters of CdO-TiO<sub>2</sub> thin films

Calcination temperature (°C)/Angle position	d		Debye-Scherrer method		Williamson-Hall method		Dislocation density
	Obs.	Calc.	D (nm)	ε	D (nm)		
<b>350</b>							
(0 0 3)	4.9711	4.9691	35.0701	-0.0002	36.19000		0.0011
(1 0 1)	4.3538	4.3521					
(0 1 2)	3.8835	3.8820					
<b>450</b>							
(0 0 3)	4.9480	4.9461	35.4458	-0.0005	32.9000		0.0010
(1 0 1)	4.3419	4.3402					
(0 1 2)	3.8738	3.8723					
<b>550</b>							
(0 0 3)	4.9845	4.9825	36.1534	-0.0001	38.0947		0.00103
(1 0 1)	4.3696	4.3679					
(0 1 2)	3.8949	3.8934					
<b>650</b>							
(0 0 3)	5.0040	5.0021	35.8137	-0.0003	36.1900		0.0009
(1 0 1)	4.3824	4.3807					
(0 1 2)	3.9068	3.9052					

**SEM analysis:** The influence of calcination temperature on the surface morphology of CdO-TiO<sub>2</sub> thin films was studied by scanning electron microscopy technique. Figure 2 shows the SEM images of CdO-TiO<sub>2</sub> thin films at 350, 450 and 550 and 650°C. It is clearly seen that the films have density packed structures with a homogeneous surfaces containing nanocrystalline grains. The surfaces

of CdO-TiO<sub>2</sub> thin films have porous structures and this porosity may be due to the evaporation of water molecules during the growing process and the annealing treatment. It was found that the morphology and crystalline size were increase slightly with increasing calcination temperature, this mean the the prepared thin films were stable atvarios temperature.

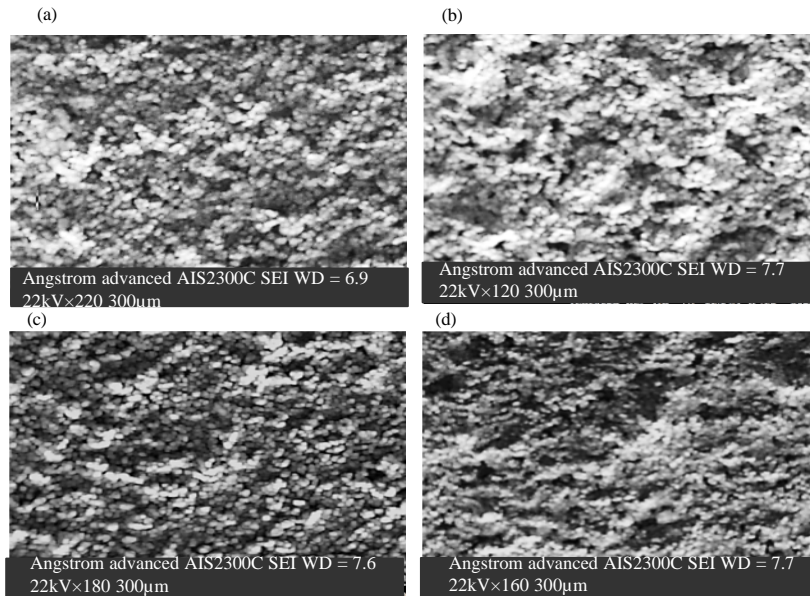


Fig. 2: SEM images of CdO-TiO<sub>2</sub> nanocomposite thin film at different temperatures (a = 350°C, b = 450°C, c = 550°C and d = 650°C)

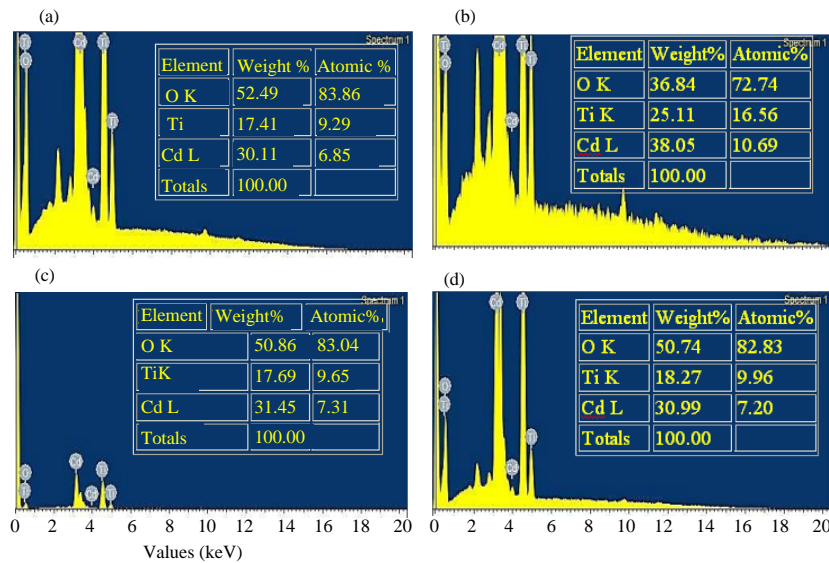


Fig. 3: EDS spectra of CdO-TiO<sub>2</sub> nanocomposite thin film at different temperatures (a = 350°C, b = 450°C, c = 550°C and d = 650°C)

**EDS analysis:** The EDS spectra of the nanocomposite CdO-TiO<sub>2</sub> thin films, weight ratio and atomic ratio compositions of Cd, Ti and O in the films at different substrates temperatures are given in Fig. 3 which show that all the films contain the elements Cd, Ti and O as expected.

**AFM analysis:** The surface morphologies of CdO-TiO<sub>2</sub> thin films were studied using Atomic Force Microscope (AFM). AFM images of the thin films calcined at 350, 450, 550 and 650°C are shown in Fig. 4. The results show

Table 3: Mean grain size and roughness of Cd-TiO<sub>2</sub> nanocomposite obtained from AFM analysis

Temperature (°C)	Mean grain size (nm)	Roughness (nm)
350	97	084.104
450	105	091.595
550	106	094.784
650	109	116.08

that increasing the calcination temperature causes the increasing of the surface roughness slightly due to increase as grain size as in Table 3. This is due to the increase in the mobility and the migration by increasing of annealing temperature.

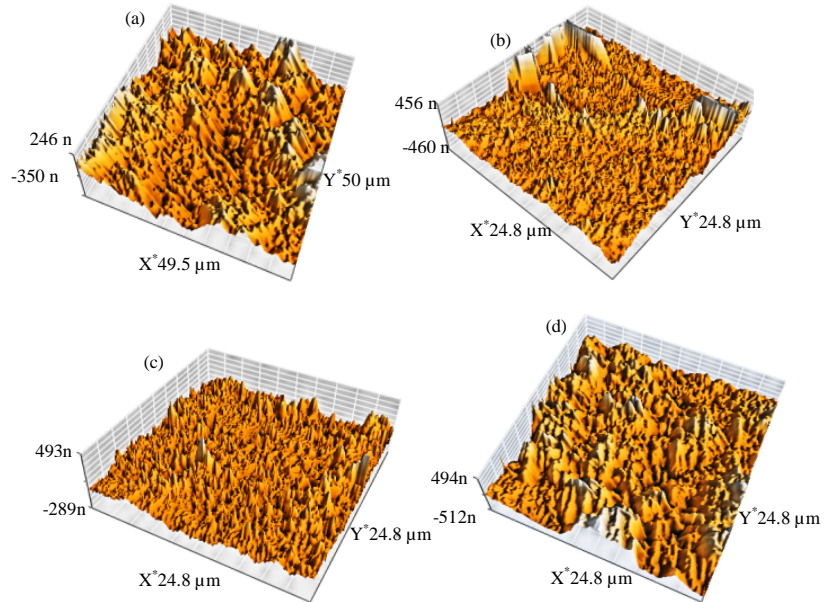


Fig. 4: AFM micrographs of CdO-TiO<sub>2</sub> nanocomposite thin films at different temperatures (a = 350°C, b = 450°C, c = 550°C and d = 650°C)

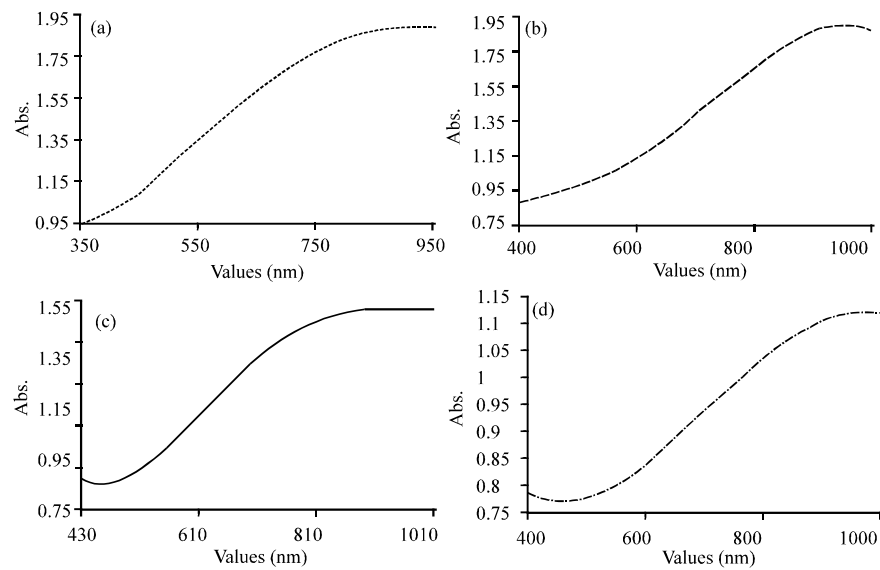


Fig. 5: Absorption spectra of CdO-TiO<sub>2</sub> nanocomposite thin films at different temperatures (a = 350°C, b = 450°C, c = 550°C and d = 650°C)

**Optical properties:** The absorption spectra and extinction coefficient of the CdO-TiO<sub>2</sub> thin films are shown in Fig. 5 and 6, respectively. The absorption spectra were obtained by using a reference glass substrate. The optical properties of CdO-TiO<sub>2</sub> thin films are illustrated in Table 4. It can be noticed from

the Fig. 6 that the absorption edge exhibits a red shift. The optical band gap of CdO-TiO<sub>2</sub> film can be determined from the absorption spectra as in Fig. 7. The absorption coefficient, ' $\alpha$ ' is related to the optical band gap  $E_g$  by the relation Eq. 1 (Chopra and Das, 1983):

Table 4 : Optical properties of CdO-TiO<sub>2</sub> nanocomposite thin films at different temperatures

Temperature (°C)	Absorption coefficient (X10 <sup>4</sup> )	Extinction coefficient	Energy gap (eV)	Optical conductivity (X10 <sup>14</sup> )	Real dielectric constant	Refractive index
350	4.52	0.30	1.25	2.72	6.13	2.49
450	4.88	0.35	2.25	2.97	6.28	2.53
550	4.11	0.31	2.05	2.56	6.60	2.58
650	2.97	0.21	0.90	1.73	5.87	2.43

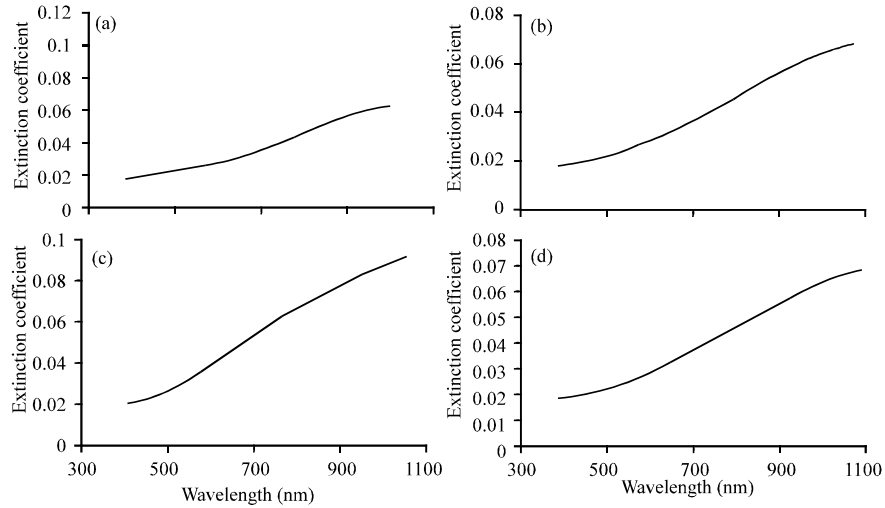


Fig. 6: Extinction coefficient of CdO-TiO<sub>2</sub> nanocomposite thin films at different temperatures (a = 350°C, b = 450°C, c = 550°C and d = 650°C)

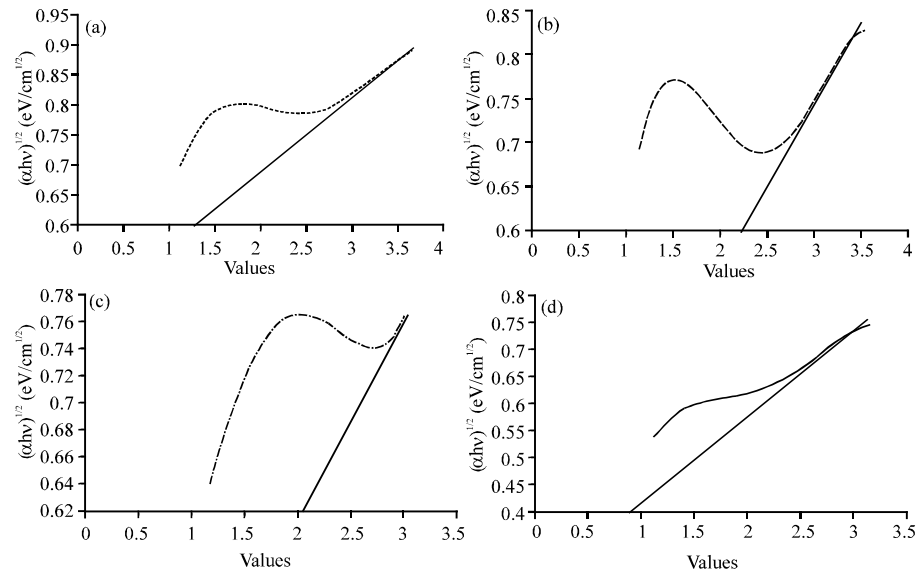


Fig. 7: Energy gaps of CdO-TiO<sub>2</sub> nanocomposite thin films at different temperatures (a = 350°C, b = 450°C, c = 550°C and d = 650°C)

$$\alpha h\nu = B(h\nu - E_g)^n \quad (1)$$

Where:

h = Plank's constant

v = The frequency of the radiation

B = A constant which depends on the nature of transition

n = A number which can take the values 1/2, 2, 3 and 3/2 or more depending on whether the transition is direct-allowed, indirect-allowed, direct-forbidden or indirect-forbidden

In the present case for the CdO-TiO<sub>2</sub> thin films, the plots of  $(\alpha hv)^{1/2}$  versus  $h\nu$  (Fig. 7) demonstrate a direct segment showing that optical transitions are indirect allowed transitions. The indirect band gap ( $E_g$ ) is dictated by extrapolating the straight-line part of the plot to the energy axis. The intercept on the energy axis gives the estimation of band gap energy for every one of the samples. The results mean that the band gap energy, decrease when the substrate temperature increase. This is because of the development of new confined levels which are proficient to get electrons and produce restricted energy tails inside the optical energy gap which take a shot at the absorption of low energy photons (deviation of the absorption edge towards lower energies) and this thusly, prompts a decreasing of the energy gap (Salman *et al.*, 2015).

### CONCLUSION

CdO-TiO<sub>2</sub> nanocomposite thin films were deposited by doctor blading method with substrate temperatures in the range from 350-650°C. The effect of substrate temperature of the CdO-TiO<sub>2</sub> thin films on the structural and optical properties was investigated. With the increase in substrate temperature, it was observed that there is a corresponding increase in grain growth and crystallinity of CdO-TiO<sub>2</sub> thin films deposited on glass substrates. The XRD spectra indicated that the films are polycrystalline rhombohedral structure. The allowed indirect band gap at the deposition temperature ranging from 350-650°C was estimated to be in the range from 1.25-0.9 eV.

### REFERENCES

- Andersson, M., L. Osterlund, S. Ljungstrom and A. Palmqvist, 2002. Preparation of nanosize anatase and rutile TiO<sub>2</sub> by hydrothermal treatment of microemulsions and their activity for photocatalytic wet oxidation of phenol. *J. Phys. Chem. B*, 106: 10674-10679.
- Benko, G., P. Myllyperkio, J. Pan, A.P. Yartsev and V. Sundstrom, 2003. Photoinduced electron injection from Ru(dcbpy)<sub>2</sub> (NCS)<sub>2</sub> to SnO<sub>2</sub> and TiO<sub>2</sub> nanocrystalline films. *J. Am. Chem. Soc.*, 125: 1118-1119.
- Burns, G. and B.A. Scott, 1973. Lattice modes in ferroelectric perovskites: PbTiO<sub>3</sub>. *Phys. Rev. B*, 7: 3088-3101.
- Burns, G. and F.H. Dacol, 1978. Lattice modes in ferroelectric perovskites, III: Soft modes in BaTiO<sub>3</sub>. *Phys. Rev. B*, 18: 5750-5750.
- Burns, G., 1974. Lattice modes in ferroelectric perovskites, II: Pb<sub>1-x</sub>Ba<sub>x</sub>TiO<sub>3</sub> including BaTiO<sub>3</sub>. *Phys. Rev. B*, 10: 1951-1959.
- Chandrasekharan, N. and P.V. Kamat, 2000. Improving the photoelectrochemical performance of nanostructured TiO<sub>2</sub> films by adsorption of gold nanoparticles. *J. Phys. Chem. B*, 104: 10851-10857.
- Chopra, K.L. and S.R. Das, 1983. Why Thin Film Solar Cells?. In: *Thin Film Solar Cells*, Chopra, K.L. and S.R. Das (Eds.). Springer, Boston, Massachusetts, USA., ISBN:978-1-4899-0420-1, pp: 1-18.
- Dakhel, A.A. and A.Y. Ali-Mohamed, 2007. Optical and transport phenomena in CdO: La films prepared by sol-gel method. *J. Sol-Gel Sci. Technol.*, 44: 241-247.
- Dakhel, A.A., 2011. Structural, optical and electrical measurements on boron-doped CdO thin films. *J. Mater. Sci.*, 46: 6925-6931.
- El-Mallah, H., B.E. Watts and B. Wanklyn, 1987. Birefringence of CaTiO<sub>3</sub> and CdTiO<sub>3</sub> single crystals as a function of temperature. *Phase Transitions A Multinational J.*, 9: 235-245.
- Gorshunov, B.P., A.V. Pronin, I. Kutskov, A.A. Volkov and V.V. Lemanov *et al.*, 2005. Polar phonons and specific features of the ferroelectric states in cadmium titanate. *Phys. Solid State*, 47: 547-555.
- Henari, F.Z. and A.A. Dakhel, 2008. Linear and nonlinear optical properties of hydrogenated CdO thin films. *Laser Phys.*, 18: 1557-1561.
- Karuppuchamy, S., K. Nonomura, T. Yoshida, T. Sugiura and H. Minoura, 2002. Cathodic electrodeposition of oxide semiconductor thin films and their application to dye-sensitized solar cells. *Solid State Ionics*, 151: 19-27.
- Kumar, A., S. Mandal, P.R. Selvakannan, R. Pasricha and A.B. Mandale *et al.*, 2003. Investigation into the interaction between surface-bound alkylamines and gold nanoparticles. *Langmuir*, 19: 6277-6282.
- Lokhande, C.D., R.R. Salunkhe, D.S. Dhawale and D.P. Dubal, 2009. Sprayed CdO thin films for Liquefied Petroleum Gas (LPG) detection. *Sens. Actuators B: Chem.*, 140: 86-91.
- Maity, R. and K.K. Chattopadhyay, 2006. Synthesis and characterization of aluminum-doped CdO thin films by sol-gel process. *Solar Energy Mater. Solar Cells*, 90: 597-606.
- Matsubara, K., P. Fons, K. Iwata, A. Yamada, K. Sakurai, H. Tampo and S. Niki, 2003. ZnO transparent conducting films deposited by pulsed laser deposition for solar cell applications. *Thin Solid Films*, 431-432: 369-372.
- Matsumoto, Y., Y. Ishikawa, M. Nishida and S. Ii, 2000. A new electrochemical method to prepare mesoporous titanium (IV) oxide photocatalyst fixed on alumite substrate. *J. Phys. Chem. B*, 104: 4204-4209.

- Peto, G., G.L. Molnar, Z. Paszti, O. Geszti and A. Beck *et al.*, 2002. Electronic structure of gold nanoparticles deposited on SiO<sub>2</sub>/Si(100). *Mater. Sci. Eng. C*, 19: 95-99.
- Rabe, K.M., C.H. Ahn and J.M. Triscone, 2007. *Physics of Ferroelectrics: A Modern Perspective*. Vol. 105, Springer, Berlin, Germany, ISBN:978-3-540-34590-9, Pages: 384.
- Rothschild, A., A. Levakov, Y. Shapira, N. Ashkenasy and Y. Komem, 2003. Surface photovoltage spectroscopy study of reduced and oxidized nanocrystalline TiO<sub>2</sub> films. *Surf. Sci.*, 532: 456-460.
- Rusu, R.S. and G.I. Rusu, 2005. On the electrical and optical characteristics of CdO thin films. *J. Optoelectron. Adv. Mater.*, 7: 823-828.
- Sakai, N., A. Fujishima, T. Watanabe and K. Hashimoto, 2001. Enhancement of the photoinduced hydrophilic conversion rate of TiO<sub>2</sub> film electrode surfaces by anodic polarization. *J. Phys. Chem. B*, 105: 3023-3026.
- Salman, S.A., Z.T. Khodair and S.J. Abed, 2015. Study the effect of substrate temperature on the optical properties of CoFe<sub>2</sub>O<sub>4</sub> films prepared by chemical spray pyrolysis method. *Intl. Lett. Chem. Phys. Astron.*, 61: 118-127.
- Sasaki, S., C.T. Prewitt, J.D. Bass and W.A. Schulze, 1987. Orthorhombic perovskite CaTiO<sub>3</sub> and CdTiO<sub>3</sub>: Structure and space group. *Acta Crystallogr. Sect. C Crystal Struct. Commun.*, 43: 1668-1674.
- Shan, Y.J., H. Mori, R. Wang, W. Luan and H. Imoto *et al.*, 2001. Powder X-ray diffraction study of ferroelectric phase transition in perovskite oxide CdTiO<sub>3</sub>. *Ferroelectr.*, 259: 85-90.
- Shigenari, T., K. Abe, T. Takemoto, O. Sanaka and T. Akaike *et al.*, 2006. Raman spectra of the ferroelectric phase of SrTi<sub>1-x</sub>O<sub>3</sub>: Symmetry and domains below T<sub>c</sub> and the origin of the phase transition. *Phys. Rev. B*, Vol. 74, 10.1103/PhysRevB.74.174121
- Soon, H.P., H. Taniguchi, Y. Fujii, M. Itoh and M. Tachibana, 2008. Direct observation of the soft mode in the paraelectric phase of PbTiO<sub>3</sub> by confocal micro-Raman scattering. *Phys. Rev. B*, Vol. 78, 10.1103/PhysRevB.78.172103
- Srinivasaraghavan, R., R. Chandiramouli, B.G. Jeyapragash and S. Seshadri, 2013. Quantum chemical studies on CdO nanoclusters stability. *Spectrochim. Acta Part A Mol. Biomol. Spectrosc.*, 102: 242-249.
- Sun, P.H., T. Nakamura, Y.J. Shan, Y. Inaguma and M. Itoh, 1998. The study on the dielectric property and structure of Perovskite Titanate CdTiO<sub>3</sub>. *Ferroelectr.*, 217: 137-145.
- Takeda, S., S. Suzuki, H. Odaka and H. Hosono, 2001. Photocatalytic TiO<sub>2</sub> thin film deposited onto glass by DC magnetron sputtering. *Thin Solid Films*, 392: 338-344.
- Takesada, M., M. Itoh and T. Yagi, 2006. Perfect softening of the ferroelectric mode in the isotope-exchanged strontium Titanate of SrTiO<sub>3</sub> 18 studied by light scattering. *Phys. Rev. Lett.*, Vol. 96, 10.1103/PhysRevLett.96.227602
- Taniguchi, H., M. Itoh and T. Yagi, 2007. Ideal soft mode-type quantum phase transition and phase coexistence at quantum critical point in O<sub>18</sub>-exchanged SrTiO<sub>3</sub>. *Phys. Rev. Lett.*, 99: 017602-017602.
- Taniguchi, H., T. Yagi, M. Takesada and M. Itoh, 2005. Isotope effect on the soft-mode dynamics of SrTiO<sub>3</sub> studied by Raman scattering. *Phys. Rev. B*, Vol. 72,
- Uplane, M.D., B.J. Lokhande and P.S. Patil, 2004. Studies on cadmium oxide sprayed thin films deposited through non-aqueous medium. *Mater. Chem. Phys.*, 84: 238-242.
- Wang, R., K. Hashimoto, A. Fujishima, M. Chikuni and E. Kojima *et al.*, 1997. Light-induced amphiphilic surfaces. *Nature*, 388: 431-432.
- Watanabe, T., A. Nakajima, R. Wang, M. Minabe and S. Koizumi *et al.*, 1999. Photocatalytic activity and photoinduced hydrophilicity of titanium dioxide coated glass. *Thin Solid Films*, 351: 260-263.
- Zhang, W., Y. Li, S. Zhu and F. Wang, 2004. Influence of argon flow rate on TiO<sub>2</sub> photocatalyst film deposited by dc reactive magnetron sputtering. *Surface Coat. Technol.*, 182: 192-198.